



UNIVERSITÀ DI PISA

Electromagnetic Radiations and Biological Interactions

***“Laurea Magistrale” in Biomedical Engineering
First semester (6 credits, 60 hours), academic year 2011/12***

***Prof. Paolo Nepa
p.nepa@iet.unipi.it***

Electromagnetic Characterization of Biological Tissues

Edited by Dr. Anda Guraliuc

17/11/2011



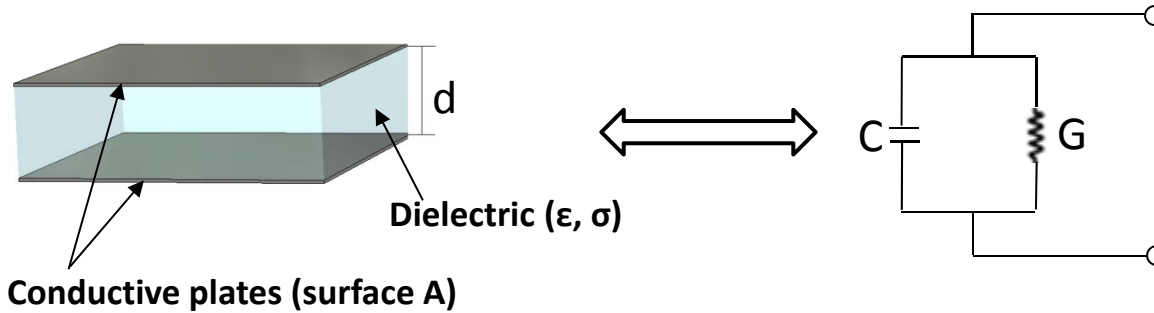
Lecture Content

- **Tissue EM characterization: complex permittivity**
 - **Frequency dependence: Debye Model**
 - **Frequency dependence: Cole-Cole Model**
- **Complex permittivity of some biological tissues**
 - **Applications**

Introduction

- The study of dielectric properties of tissues were investigated by the need for such information in electromagnetic dosimetry (dosimetry deals with the simulation of electromagnetic exposure situations and the calculation of internal fields within exposed structures).
- Dielectric properties of diseased and normal tissues can differ significantly at microwave frequencies (for example, the development of microwave breast cancer detection and treatment has been driven by reports on substantial contrast in the dielectric properties of malignant and normal breast tissues)

Static fields (steady state)



Dielectric=air \implies Electric displacement: $D = \frac{\epsilon_0 V}{d}$

$\epsilon_0 = 8.85 \times 10^{-12} \text{ F/m}$

Charge (Gauss's law): $Q = \epsilon_0 A \frac{V}{d} \implies$ Capacitance: $C_0 = \frac{Q}{V} = \frac{\epsilon_0 A}{d}$

Dielectric (ϵ, σ) \implies $\underline{D} = \epsilon_0 \underline{E} + \underline{P}$ \rightarrow dielectric polarization vector $\underline{P} = \chi \epsilon_0 \underline{E}$

electric field vector \underline{E} \rightarrow Electric susceptibility χ

$\underline{D} = \epsilon_0 \underline{E} + \chi \epsilon_0 \underline{E} = \epsilon_0 (1 + \chi) \underline{E}$

relative permittivity of the material: ϵ_r

$C = \epsilon_0 \epsilon_r \frac{A}{d} = \epsilon_r C_0$

static relative permittivity

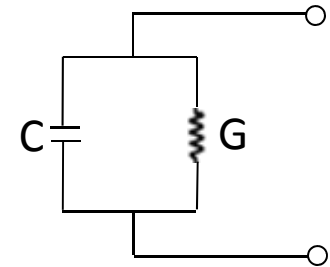
static conductivity

In the equivalent circuit we have an electrical conductance: $G = \sigma_s \frac{A}{d}$ $\left(R = 1/G = \frac{1}{\sigma_s} \frac{d}{A} \right)$

Complex permittivity (quasi-static case)

What happens for sinusoidal excitation ?

At low frequency (quasi static condition): the equivalent circuit presents a complex admittance that can be derived from the static model



$$Y = I / V = G + j\omega C = \frac{\sigma_s A}{d} + j\omega \epsilon_0 \epsilon_r \frac{A}{d} = \frac{A}{d} (\sigma_s + j\omega \epsilon_0 \epsilon_r)$$

$$Y = I / V = j\omega \frac{\epsilon_0 A}{d} \left(\epsilon_r - j \frac{\sigma_s}{\omega \epsilon_0} \right) = j\omega C_0 \tilde{\epsilon}$$

$$\tilde{\epsilon} = \epsilon_r - j \frac{\sigma_s}{\omega \epsilon_0} \quad (= \epsilon' - j\epsilon'') \rightarrow \text{material complex permittivity}$$

Complex permittivity at higher frequencies

The same model can be extended to higher frequencies:

$$Y = I/V = j\omega C_0 \tilde{\varepsilon} \quad \tilde{\varepsilon} = \varepsilon' - j\varepsilon'' \rightarrow \text{material complex permittivity at } \omega$$

$$\left(\tilde{\varepsilon} = \varepsilon' - j\varepsilon'' = \varepsilon'(1 - j\varepsilon''/\varepsilon') = \varepsilon'(1 - j \tan \delta) \right) \text{ (Loss tangent)}$$

As an alternative:

$$\tilde{\varepsilon}(\omega) = \varepsilon' - j\varepsilon'' = \varepsilon' - j \frac{\sigma}{\omega \varepsilon_0} \quad \sigma = \omega \varepsilon_0 \varepsilon'' \rightarrow \text{material complex conductivity at } \omega$$

$$\text{In the limit of low frequency: } \tilde{\varepsilon} = \varepsilon' - j \frac{\sigma}{\omega \varepsilon_0} \rightarrow \varepsilon_r - j \frac{\sigma_s}{\omega \varepsilon_0}$$

$\tilde{\varepsilon}(\omega), \varepsilon'(\omega), \varepsilon''(\omega), \sigma(\omega)$: they are frequency dependent

$$D(\omega) = \varepsilon_0 (\varepsilon' - j\varepsilon'') E(\omega) = \left(\varepsilon' - j \frac{\sigma}{\omega \varepsilon_0} \right) E(\omega) = \varepsilon_0 \tilde{\varepsilon}(\omega) E(\omega)$$

(Note: for an isotropic medium, vector amplitude only can be considered)

Debye Model (time domain response)

$$D(\omega) = \varepsilon_0 \tilde{\varepsilon}(\omega) E(\omega) \quad \text{A time-invariant linear system with a frequency response } \varepsilon_0 \tilde{\varepsilon}(\omega)$$

When a material is exposed to an electric field, its response assumes a modification of the charge density (D) due to the **electric polarization phenomena**. This process is not instantaneous and suppose that it can be described by a **first-order process characterized by a constant time τ** , namely relaxation time.

Under step-function excitation:

$$E = E_0 u(t)$$

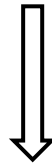
$$\left\{ \begin{array}{l} D = \left[D_\infty + (D_0 - D_\infty) \left(1 - e^{-t/\tau} \right) \right] u(t) \\ t \rightarrow 0 \Rightarrow D = D_\infty \text{ (instantaneous response)} \\ t \rightarrow \infty \Rightarrow D = D_0 \text{ (steady-state response)} \end{array} \right.$$

$$\frac{D(t)}{\varepsilon_0 E_0} = \left[\varepsilon_\infty + (\varepsilon_s - \varepsilon_\infty) \left(1 - e^{-t/\tau} \right) \right] u(t) \quad \left\{ \begin{array}{l} \varepsilon_\infty = \frac{D_\infty}{\varepsilon_0 E_0} \rightarrow \text{permittivity @ high frequency} \\ \varepsilon_s = \frac{D_0}{\varepsilon_0 E_0} \rightarrow \text{static permittivity} \end{array} \right.$$

Debye Model (frequency model)

Under step-function excitation:

$$E = E_0 u(t) \quad \Rightarrow \quad \frac{D(t)}{\varepsilon_0 E_0} = \left[\varepsilon_\infty + (\varepsilon_s - \varepsilon_\infty) (1 - e^{-t/\tau}) \right] u(t)$$



$$\left\{ \begin{array}{l} \varepsilon_\infty = \frac{D_\infty}{\varepsilon_0 E_0} \\ \varepsilon_s = \frac{D_0}{\varepsilon_0 E_0} \end{array} \right.$$

$$D(\omega) = \varepsilon_0 \tilde{\varepsilon}(\omega) E(\omega) \quad \tilde{\varepsilon}(\omega) = \varepsilon_\infty + \frac{\varepsilon_s - \varepsilon_\infty}{1 + j\omega\tau} = \varepsilon_\infty + \frac{\Delta\varepsilon}{1 + j\omega\tau}$$

$$\left\{ \begin{array}{l} \Delta\varepsilon = \varepsilon_s - \varepsilon_\infty \longrightarrow \text{dispersion amplitude} \\ \tau \longrightarrow \text{relaxation time} \end{array} \right.$$

Debye first-order model

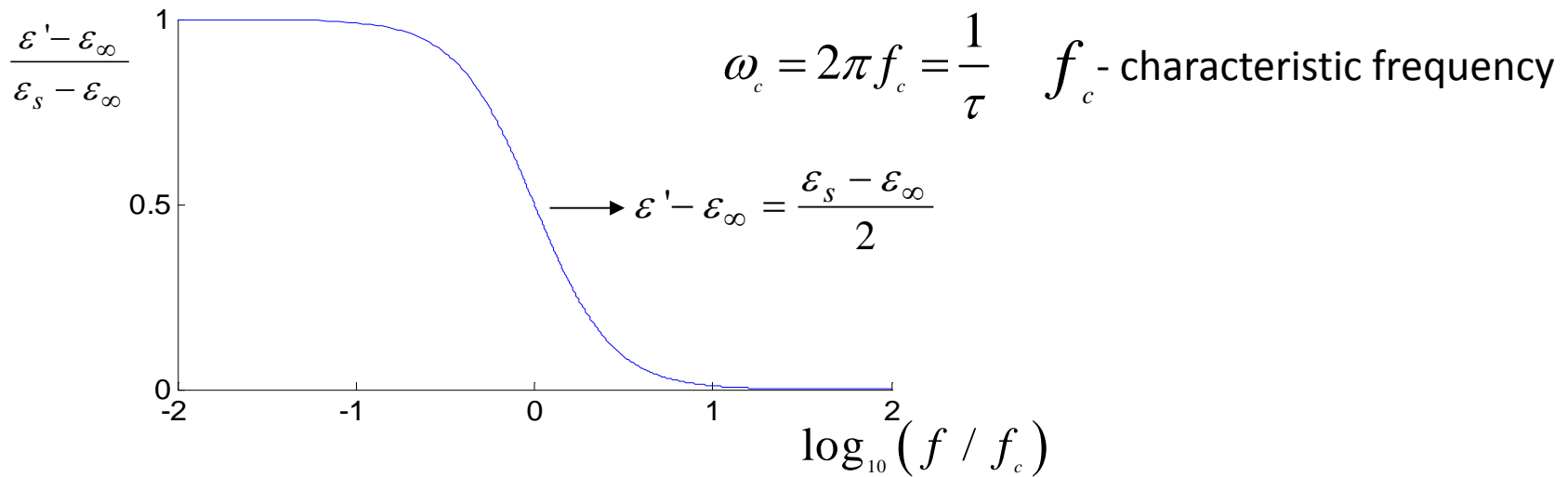
Debye Model – Real term

After adding static conductivity term \Rightarrow

$$\tilde{\epsilon} = \epsilon_{\infty} + \frac{\epsilon_s - \epsilon_{\infty}}{1 + j\omega\tau} - j \frac{\sigma_s}{\omega\epsilon_0} \quad \left(\tilde{\epsilon} = \epsilon_{\infty} + \frac{\epsilon_s - \epsilon_{\infty}}{1 + j\omega\tau} \frac{1 - j\omega\tau}{1 - j\omega\tau} - j \frac{\sigma_s}{\omega\epsilon_0} \right)$$

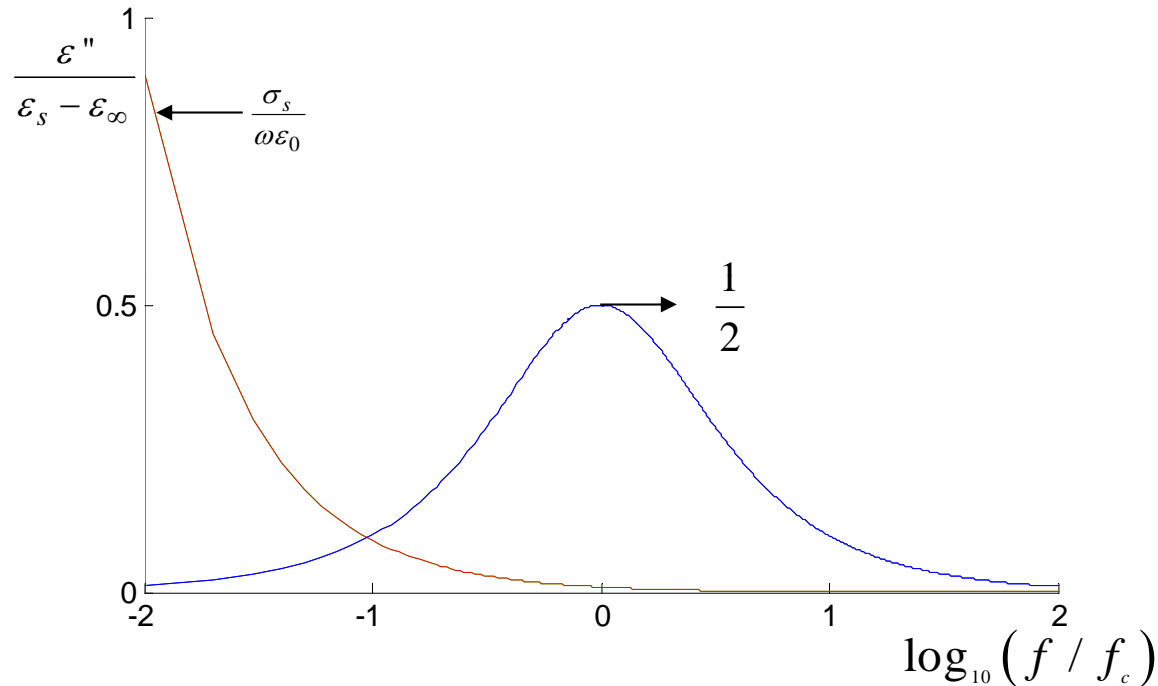
$$\Rightarrow \tilde{\epsilon} = \epsilon_{\infty} + \frac{\epsilon_s - \epsilon_{\infty}}{1 + (\omega\tau)^2} - j \left(\frac{\sigma_s}{\omega\epsilon_0} + \frac{(\epsilon_s - \epsilon_{\infty})\omega\tau}{1 + (\omega\tau)^2} \right) = \epsilon' - j\epsilon'' = \epsilon' - j \frac{\sigma}{\omega\epsilon_0}$$

$$\rightarrow \boxed{\epsilon' = \epsilon_{\infty} + \frac{\epsilon_s - \epsilon_{\infty}}{1 + (\omega\tau)^2}} \begin{cases} \omega \rightarrow \infty \Rightarrow \epsilon' \rightarrow \epsilon_{\infty} \\ \omega \rightarrow 0 \Rightarrow \epsilon' \rightarrow \epsilon_s \end{cases} \begin{array}{l} \text{Dipoles follow the applied electric field direction at} \\ \text{low frequencies and slow at high frequencies due to} \\ \text{the relaxation phenomena.} \end{array}$$



Debye Model – Imaginary term

$$\epsilon'' = \frac{\sigma_s}{\omega\epsilon_0} + \frac{(\epsilon_s - \epsilon_\infty)\omega\tau}{1 + (\omega\tau)^2}$$
 It measures relaxation losses due to the dipoles oscillations. @ f_c maximum relaxation losses.
 Neglecting the static conductivity, $\epsilon'' \rightarrow 0$ for both $\omega \rightarrow \infty$ & $\omega \rightarrow 0$



$$\epsilon'' = \frac{\sigma}{\omega\epsilon_0} \rightarrow \sigma = \omega\epsilon_0\epsilon'' = \sigma_s + \frac{(\epsilon_s - \epsilon_\infty)\epsilon_0\omega^2\tau}{1 + (\omega\tau)^2} \Rightarrow \boxed{\sigma = \sigma_s + \frac{(\sigma_\infty - \sigma_s)(\omega\tau)^2}{1 + (\omega\tau)^2}}$$

$$\sigma_s + (\epsilon_s - \epsilon_\infty)\epsilon_0/\tau = \sigma_\infty$$

Dispersion Model for Biological Tissues

In most biological tissues there are more than polarization phenomena and each one is characterized by its own relaxation time τ_i .

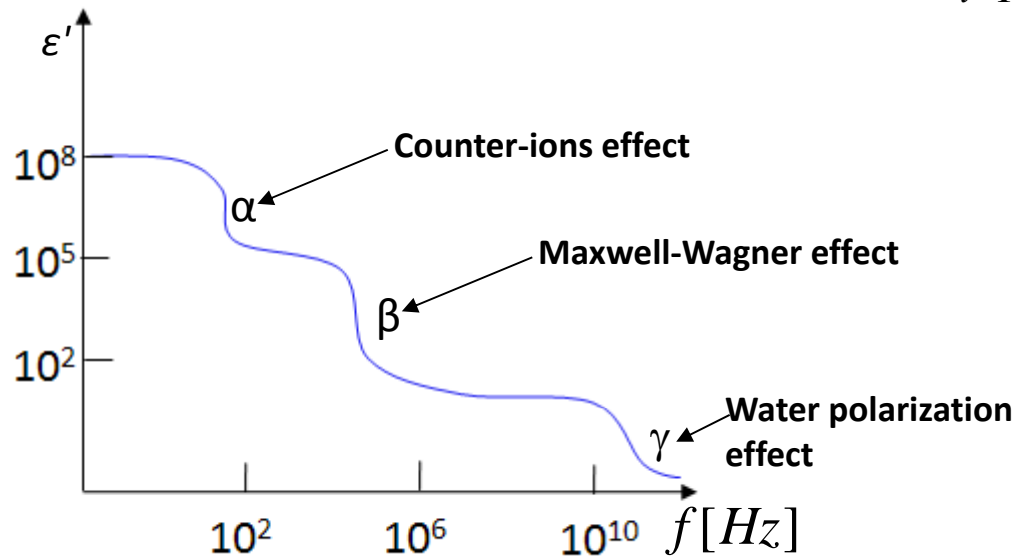
Assuming:

$$\tau_1 \ll \tau_2 \ll \tau_3 \dots \ll \tau_n$$

The biological tissue response at an electrical field $E = E_0 u(t)$ is described as a superposition of first order processes:

$$\frac{D(t)}{\varepsilon_0 E_0} = \left[\varepsilon_\infty + \Delta\varepsilon_1 \left(1 - e^{-t/\tau_1}\right) + \Delta\varepsilon_2 \left(1 - e^{-t/\tau_2}\right) + \dots + \Delta\varepsilon_n \left(1 - e^{-t/\tau_n}\right) \right] u(t)$$

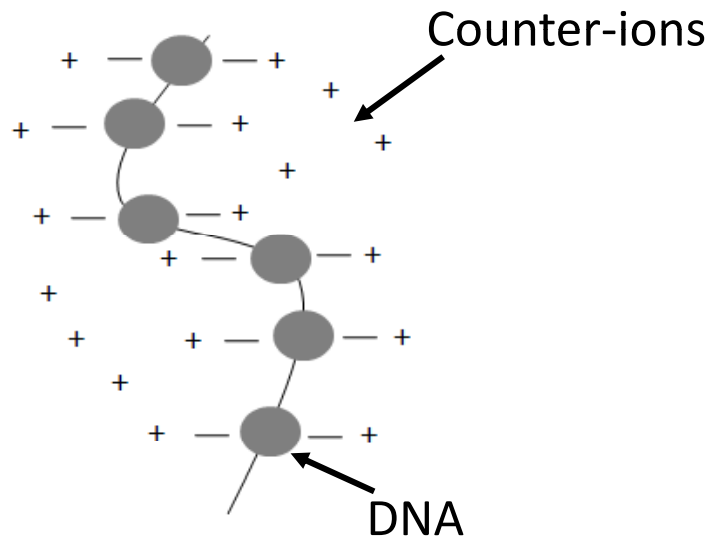
$$\tilde{\varepsilon}(\omega) = \varepsilon_\infty + \frac{\Delta\varepsilon_1}{1 + j\omega\tau_1} + \frac{\Delta\varepsilon_2}{1 + j\omega\tau_2} + \dots + \frac{\Delta\varepsilon_n}{1 + j\omega\tau_n} = \varepsilon_\infty + \sum_{i=1}^n \frac{\Delta\varepsilon_i}{1 + j\omega\tau_i} \quad \left(-j \frac{\sigma_s}{\omega\varepsilon_0} \text{ to be added}\right)$$



α - Relaxation

Polarization due to counter-ions diffusion

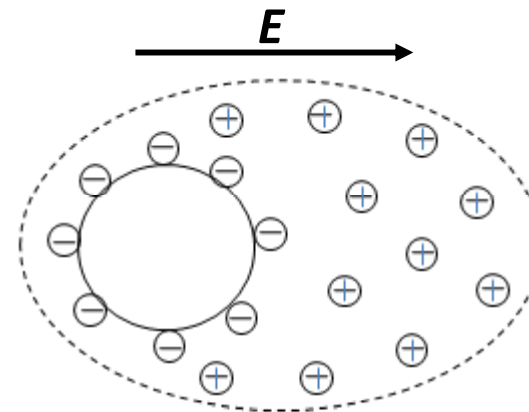
It creates an electrical double layer surrounding charged particles



In presence of an external field, the system is polarized and the counter-ions rearrange on the particle. When there is no electric field, the counter-ions tend to recover their position (controlled diffusion) with a time:

$$\tau = \frac{a^2 e}{2\mu kT}$$

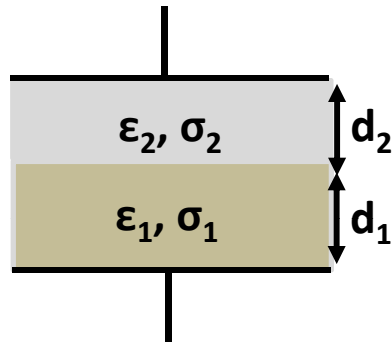
a - particle radius
 e - elementary charge ($1.6 \times 10^{-19} \text{C}$)
 μ - ion mobility [$\text{m}^2/\text{V}\cdot\text{s}$]
 k - Boltzmann constant ($1.38 \times 10^{-23} \text{J/K}$)



β - Relaxation

Interface polarization (Maxwell-Wagner effect)

Occurs in all systems where the electric current must pass through an interface between two different dielectrics.

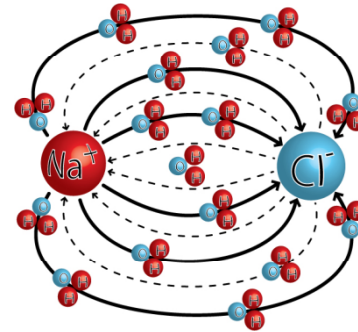
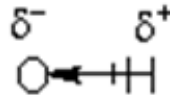
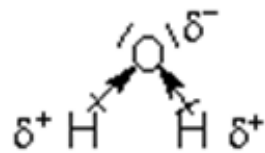


When an electric field is applied, at the separation surface between the two materials appears a dipole moment due to a different charge accumulation at both sides of the interface. This dipole moment will contribute to the dielectric constant formulation.

With the relaxation of this phenomena, the induced dipole moment at the separation of two different media, the molecules can no longer follow the field, due to a huge increase in its frequency. This relaxation can be described by the Debye or Cole-Cole models.

γ - Relaxation

Water polarization effect



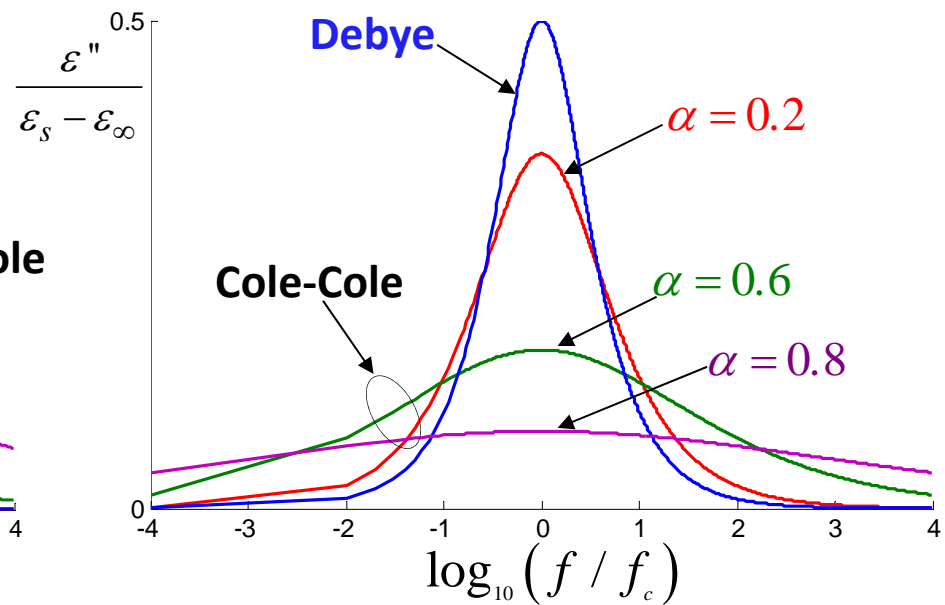
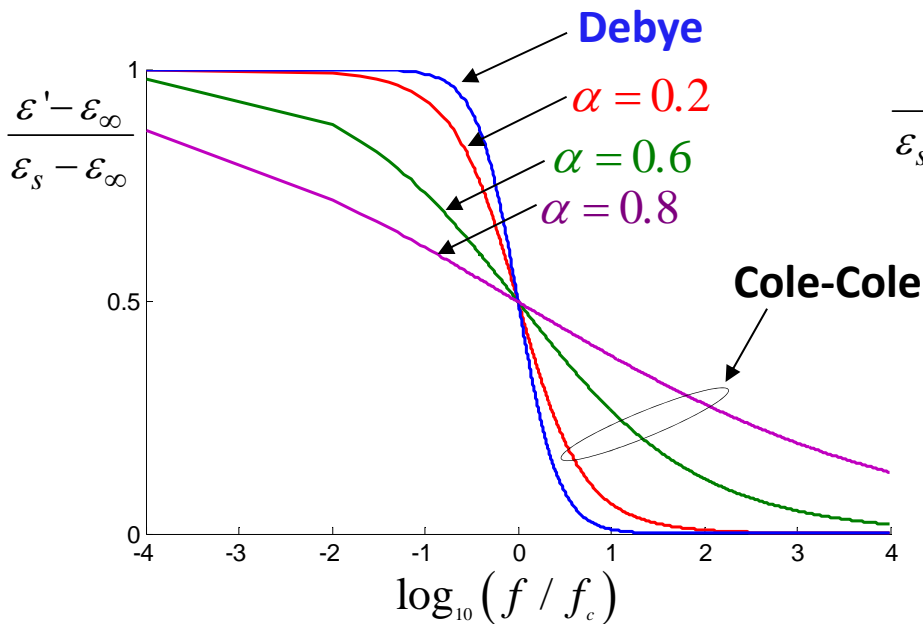
Water molecules present permanent dipoles casual oriented. When an electric field is applied, they will follow the field direction. In the absence of the external field, the permanent dipoles will relax.

Cole-Cole Model

The Cole-Cole model takes into account polarization phenomena with different characteristics, but with close relaxation times (different relaxation phenomena at close frequencies).

$$\tilde{\epsilon}(\omega) = \epsilon_{\infty} + \sum_{i=1}^n \frac{\Delta\epsilon_i}{1 + (j\omega\tau_i)^{(1-\alpha_i)}} - j \frac{\sigma_s}{\omega\epsilon_0} \rightarrow \text{Cole-Cole equation}$$

α - distribution parameter



Dielectric properties tissues – spectrum overview

- Many studies were performed over the time (see *Dimbylow* 1996), and man and animal correct anatomically model were provided, with more than 30 identified tissue types.
- Using these models for electromagnetic dosimetry requires that dielectric properties be allocated to the various tissues at all frequencies to which the model is exposed.
- *Gabriel et al* provided in 1996 a set of measurements data on the dielectric properties of biological tissues in the frequency range 10Hz to 100GHz. The spectrum from 10Hz to 100GHz was modeled to four dispersion regions. The frequency dependence within each region was expressed as a Cole-Cole term.

Biological tissues – water content

➤ For biological tissues, the most important element for their dielectric properties is water, which is about 70% of the weight of the human body. The characteristics of various biological tissues are correlated with the contained percentage of water.

There are biological tissues with:

- more than 80% water (cerebrospinal fluid, blood)
- less than 80% water (liver, skin, muscle)
- less than 40% water (bones, fat)

Where can I find biological tissue dielectric parameters?

Dielectric Properties of Body Tissues in the frequency range 10 Hz - 100 GHz

Italian National Research Council - Institute for Applied Physics "Nello Carrara" - Florence (Italy):
<http://niremf.ifac.cnr.it/tissprop/htmlclie/htmlclie.htm>

ALL TISSUES, SINGLE FREQUENCY

| | |
|---|---------|
| Type in the frequency, adjust preferences and press Go! | Go! |
| Frequency [Hz]: | 1000000 |

Format output data as:

HTML table Preformatted (fixed pitch) text

| | |
|--|---|
| Display: | <input checked="" type="checkbox"/> Tissue name |
| <input type="checkbox"/> Frequency | <input checked="" type="checkbox"/> Conductivity |
| <input checked="" type="checkbox"/> Permittivity | <input checked="" type="checkbox"/> Loss tangent |
| <input checked="" type="checkbox"/> Wavelength | <input checked="" type="checkbox"/> Penetration depth |

SINGLE TISSUE, SINGLE FREQUENCY

| | |
|--|---------|
| Type in the data, adjust preferences and press Go! | Go! |
| Tissue: | Air |
| Frequency [Hz]: | 1000000 |

Format output data as:

HTML table Preformatted (fixed pitch) text

| | |
|--|---|
| Display: | <input type="checkbox"/> Tissue name |
| <input type="checkbox"/> Frequency | <input checked="" type="checkbox"/> Conductivity |
| <input checked="" type="checkbox"/> Permittivity | <input checked="" type="checkbox"/> Loss tangent |
| <input checked="" type="checkbox"/> Wavelength | <input checked="" type="checkbox"/> Penetration depth |

SINGLE TISSUE, FREQUENCY RANGE

| | | |
|--|---|------------------------------------|
| Type in the data, adjust preferences and press Go! | Go! | |
| Tissue: | Air | |
| Start frequency [Hz]: | 10 | |
| Stop frequency [Hz]: | 100e9 | |
| Mode | Linear frequency scale (enter the number of intervals) | <input type="radio"/> 100 |
| | Logarithmic frequency scale (enter the number of values per decade) | <input checked="" type="radio"/> 5 |

Format output data as:

HTML table Preformatted (fixed pitch) text

| | |
|--|---|
| Display: | <input type="checkbox"/> Tissue name |
| <input checked="" type="checkbox"/> Frequency | <input checked="" type="checkbox"/> Conductivity |
| <input checked="" type="checkbox"/> Permittivity | <input checked="" type="checkbox"/> Loss tangent |
| <input checked="" type="checkbox"/> Wavelength | <input checked="" type="checkbox"/> Penetration depth |

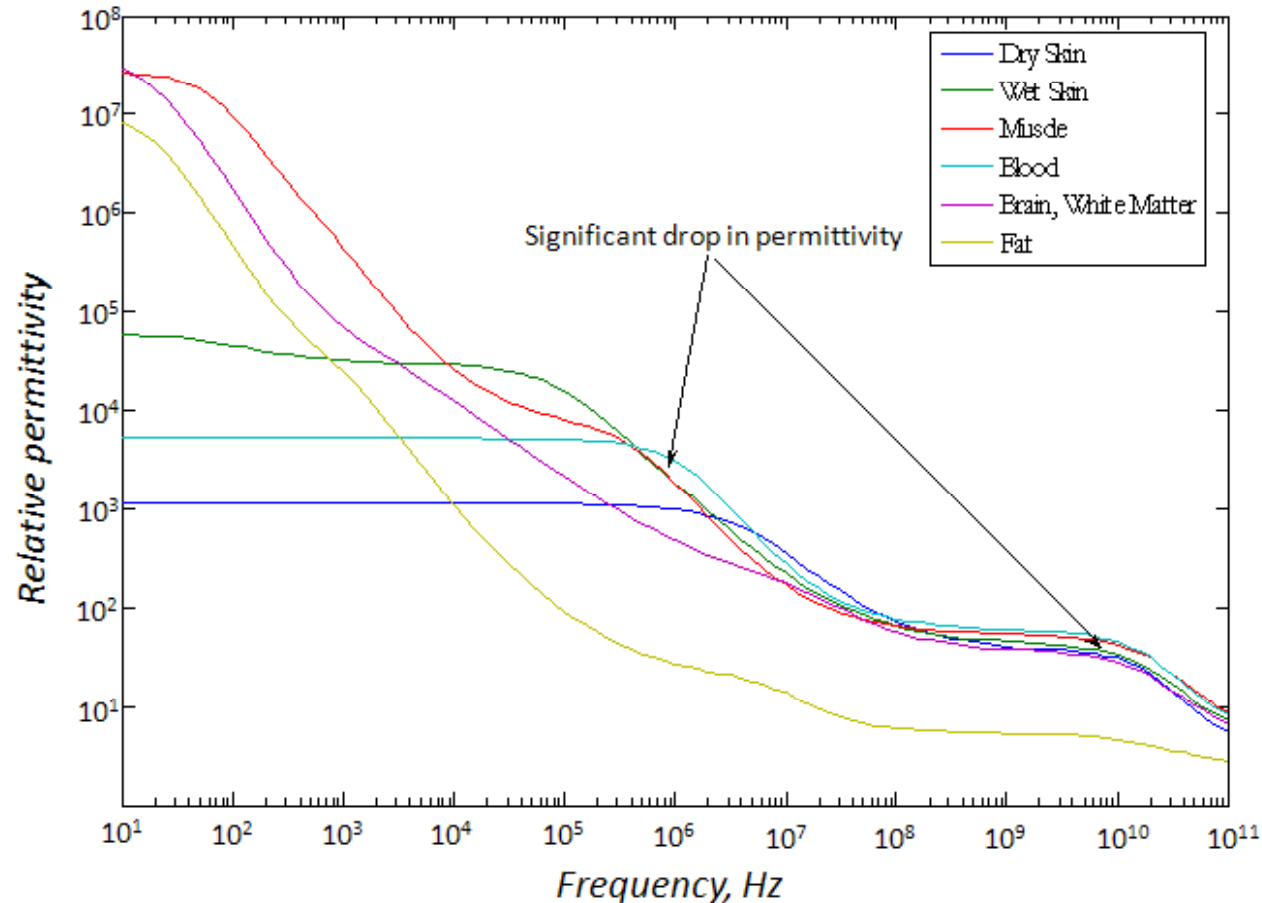
SINGLE TISSUE, SINGLE FREQUENCY

Blood @ 2400000000 Hz

| Conductivity [S/m] | Relative permittivity | Loss tangent | Wavelength [m] | Penetration depth [m] |
|--------------------|-----------------------|--------------|----------------|-----------------------|
| 2.5024 | 58.347 | 0.32123 | 0.016151 | 0.016407 |

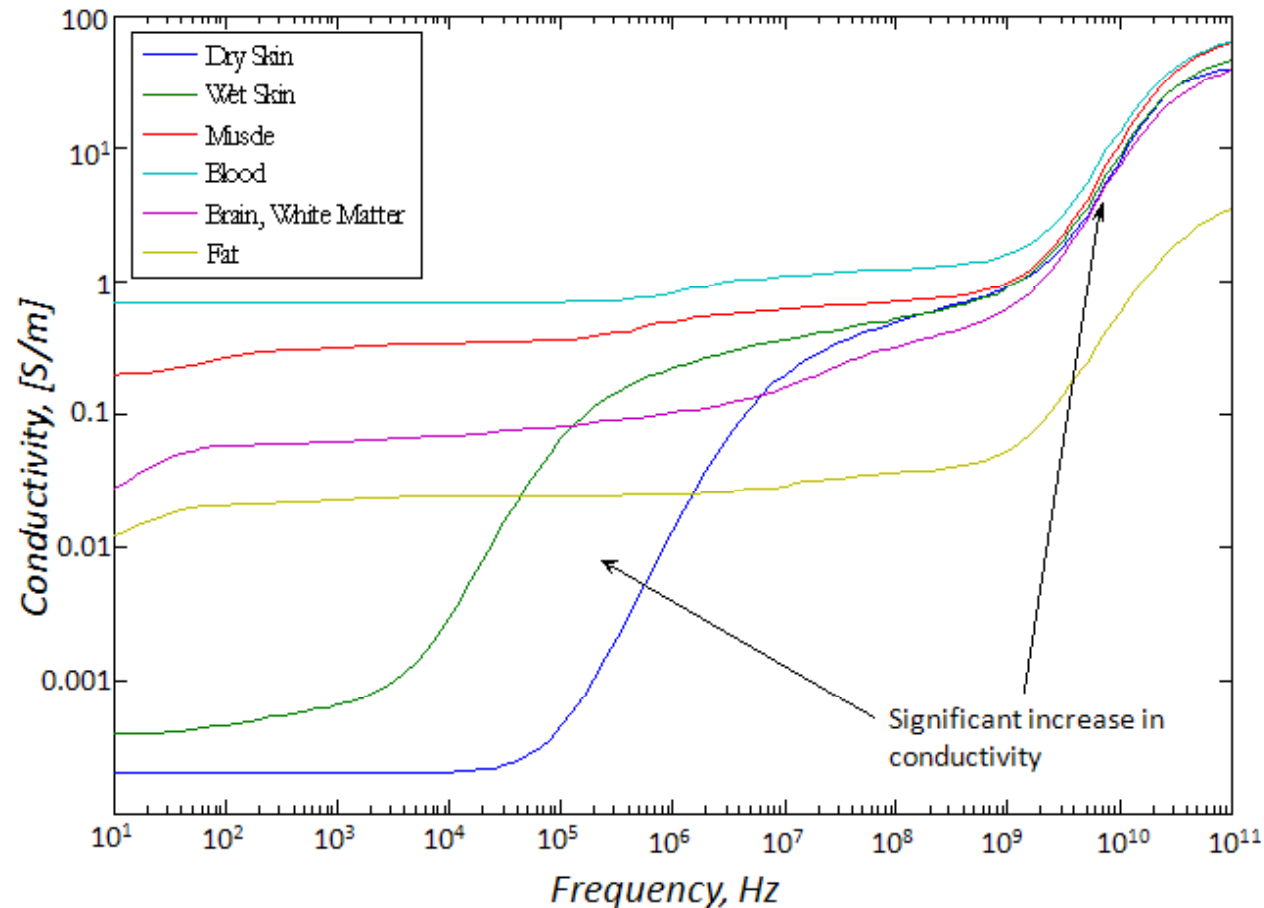
<http://www.fcc.gov/fcc-bin/dielec.sh> (Federal Communications Commission _US The tissue dielectric parameters are computed according to the 4-Cole-Cole Model described in "COMPILATION OF THE DIELECTRIC PROPERTIES OF BODY TISSUES AT RF AND MICROWAVE FREQUENCIES" by Camelia Gabriel in the U.S. Air Force Report AFOSR-TR-96

Relative Permittivity vs. Frequency for Six Different Biological Tissues



- The relative permittivity decreases when the frequency increases.
- For high water content tissues, see dry/wet skin and blood, it can not be seen the α -relaxation. The cellular structure is such as to minimize the α -relaxation. Increasing the frequency the β and γ relaxations are visible.
- For the other tissues the presence of all three relaxation processes is noticed.
- For tissues with more than 40% water content, at high frequencies, the relative permittivity shows higher values.
- At lower frequencies, tissues with high water content (more than 80% - blood) present lower relative permittivity values with respect to the lower water content tissues like muscle, brain, fat.

Conductivity vs. Frequency for Six Different Biological Tissues



- The conductivity increases when the frequency increases.
- For high water content tissue, see blood, it can be seen that the conductivity presents higher values than other tissues.
- A significant conductivity increase can be noticed at high frequencies.
- The muscle conductivity values are one order higher than the fat values, because the polarization phenomena and conduction are strongly determined by the water content.

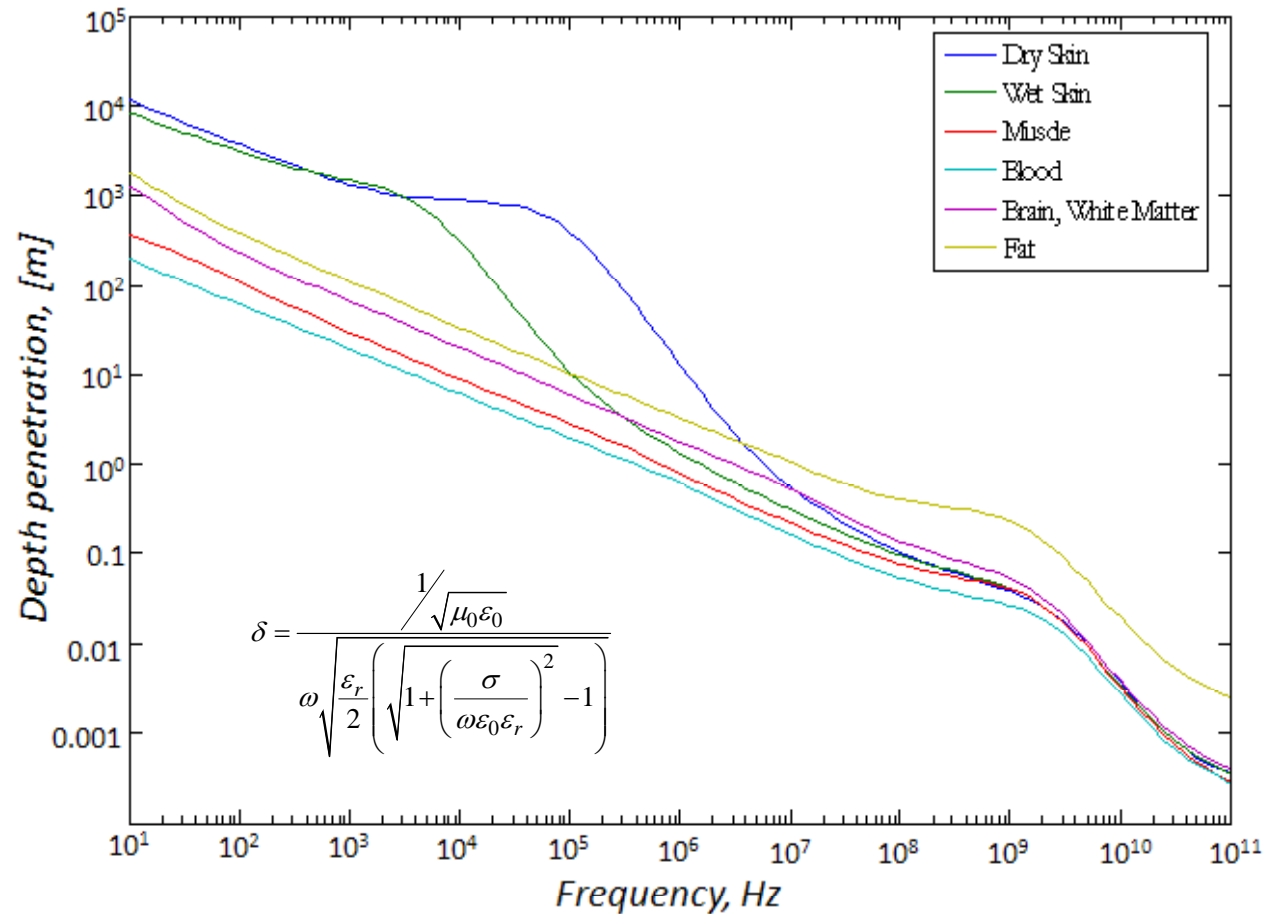
Magnetic permeability: μ

- Permeability, μ , is analogous to the permittivity in that it describes the relationship between the magnetic dipole vector and the magnetic field

$$\underline{B} = \mu \underline{H}$$

- Most of the cells and tissues that will be studied are non-magnetic
- For these types of materials, μ is considered to be equivalent to μ_0 (free space permeability)
- It is, therefore, much less critical to our analysis of EM interaction with biological tissue than permittivity and conductivity

Penetration Depth vs. Frequency for Six Different Biological Tissues



- The penetration depth decreases when the frequency increases.
- For low water content tissues (fat) the penetration depth is higher than high water content tissues (blood).

Dielectric properties of human liver tissue

- Radiofrequency, cryoablation and microwave ablation have become an alternative treatment for hepatic malignancies by producing localized hyperthermia and destroying the cancerous tissue.
- Since the distribution of absorbed electromagnetic energy depends on the ratios of electrical conductivity between the different tissues involved, quantification of conductivity of normal and malignant tissue is necessary to accurately determine energy deposition.
- In the microwave ablation (MWA) a microwave antenna is inserted into the liver tumor and power is delivered to induce cellular coagulation necrosis of the tumor and a margin of the surrounding liver tissue.

Study: • *in-vivo* and *ex-vivo* normal, malignant and cirrhotic human liver tissues were characterized from 0.5-20GHz using an open-ended coaxial probe technique.

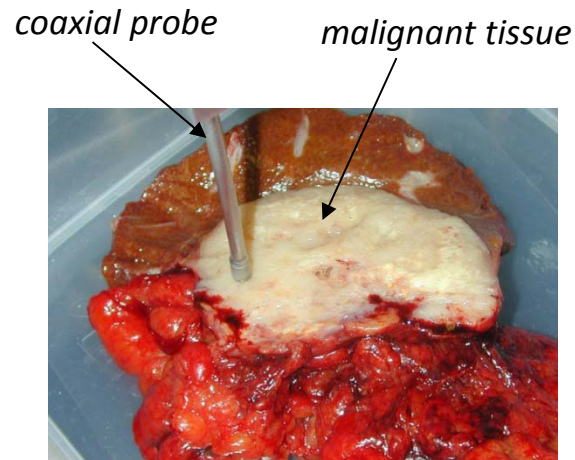
- comparison between narrowband (915MHz and 2.45GHz) and wideband (0.5-20GHz) tissue characterization.

✓ relevant to current hepatic microwave applications which use ISM-band frequencies (915MHz & 2.45GHz).

✓ characterize important microwave dielectric relaxation processes.
✓ provide dielectric properties data at a large number of frequencies.

Materials

- 6 patients with hepatocellular cancer (HCC) or hepatic metastases were considered. *In-vivo* measurements were performed on each tissue type (normal, cirrhotic and malignant) identified by the surgeon. After resection, measurements were repeated *ex vivo*.

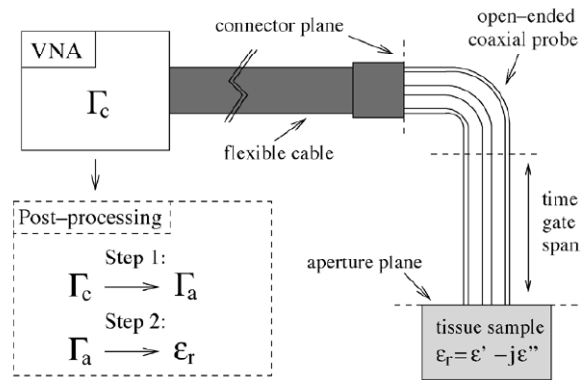


Summary of measurement numbers for the six patients

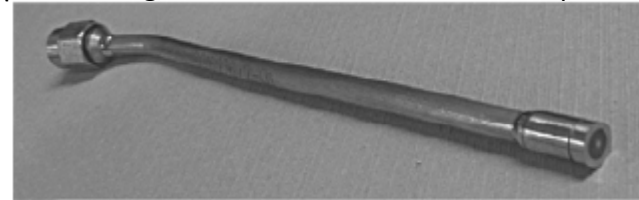
| Patient no. | <i>In vivo</i> measurements | | | <i>Ex vivo</i> measurements | | | Cancer type |
|--------------|-----------------------------|-----------|-----------|-----------------------------|-----------|-----------|---------------|
| | Normal | Malignant | Cirrhotic | Normal | Malignant | Cirrhotic | |
| 1 | 0 | 3 | 3 | 0 | 3 | 3 | Primary HCC |
| 2 | 3 | 3 | 0 | 4 | 3 | 0 | Squamous cell |
| 3 | 3 | 3 | 0 | 0 | 0 | 0 | Pancreatic |
| 4 | 0 | 0 | 0 | 4 | 3 | 0 | Colorectal |
| 5 | 3 | 3 | 0 | 12 | 15 | 0 | Colorectal |
| 6 | 2 | 2 | 0 | 0 | 0 | 0 | Colorectal |
| Total | 11 | 14 | 3 | 20 | 24 | 3 | |

Methodology

- Reflection coefficient was registered by a VNA using an open-ended coaxial probe in direct contact with the tissue under test in the frequency range 0.5-20GHz.
- Tissues dielectric properties were calculated using post-processing steps (see [9] Popovic et al, 2005).



Open-ended coaxial probe
(10-cm long and 4 mm in diameter at the aperture)



- Step1: measure reflection coefficients*
Step2: use analytical methods to correlate reflection coefficients to the dielectric tissue parameters (relative permittivity and conductivity)

$$\left(\Gamma(\omega) = \frac{Z(\omega, \varepsilon(\omega)) - R_0}{Z(\omega, \varepsilon(\omega)) + R_0} \right)$$

- Step3: fit data with the Cole-Cole model*

<http://cp.literature.agilent.com/litweb/pdf/5989-0222EN.pdf>

Single frequency data analysis – 915MHz & 2.45GHz

Average and standard deviation values for the relative permittivity and effective conductivity

In vivo

| | Normal (<i>n</i> = 11) | | Malignant (<i>n</i> = 14) | | Cirrhotic (<i>n</i> = 3) | |
|----------|-------------------------|-------------------------------|----------------------------|-------------------------------|---------------------------|-------------------------------|
| | ϵ_r | σ (S m ⁻¹) | ϵ_r | σ (S m ⁻¹) | ϵ_r | σ (S m ⁻¹) |
| 915 MHz | 59.94 ±3.05 | 1.16 ±0.14 | 64.09 ±3.78 | 1.34 ±0.13 | 61.77 2.58 | 1.38 ±0.15 |
| 2.45 GHz | 57.55 ±3.92 | 1.95 ±0.18 | 62.44 ±3.18 | 2.18 ±0.13 | 61.26 ±2.70 | 2.21 ±0.17 |

Ex vivo

| | Normal (<i>n</i> = 20) | | Malignant (<i>n</i> = 24) | | Cirrhotic (<i>n</i> = 3) | |
|----------|-------------------------|-------------------------------|----------------------------|-------------------------------|---------------------------|-------------------------------|
| | ϵ_r | σ (S m ⁻¹) | ϵ_r | σ (S m ⁻¹) | ϵ_r | σ (S m ⁻¹) |
| 915 MHz | 48.11 ±7.67 | 0.81 ±0.15 | 57.09 ±3.00 | 1.05 ±0.07 | 51.60 ±2.69 | 0.94 ±0.07 |
| 2.45 GHz | 45.79 ±7.53 | 1.68 ±0.27 | 54.88 ±3.10 | 1.99 ±0.11 | 50.16 ±2.36 | 1.83 ±0.11 |

n: number of data samples

Normal liver tissue:

$$\epsilon_{r_{iv}} > \epsilon_{r_{ev}} \text{ (25\%)}$$

$$\sigma_{iv} > \sigma_{ev} \text{ (43\% @ 915MHz)}$$

$$\sigma_{iv} > \sigma_{ev} \text{ (16\% @ 2.45GHz)}$$

Malignant liver tissue:

$$\sigma_{iv} > \sigma_{ev} \text{ (28\% @ 915MHz)}$$

@915MHz:

$$\sigma_{iv_malignant} > \sigma_{iv_normal} \text{ (16\%)}$$

$$\epsilon_{r_{ev_malignant}} > \epsilon_{r_{ev_normal}} \text{ (19\%)}$$

$$\sigma_{ev_malignant} > \sigma_{ev_normal} \text{ (30\%)}$$

@2.45GHz:

$$\epsilon_{r_{ev_malignant}} > \epsilon_{r_{ev_normal}} \text{ (20\%)}$$

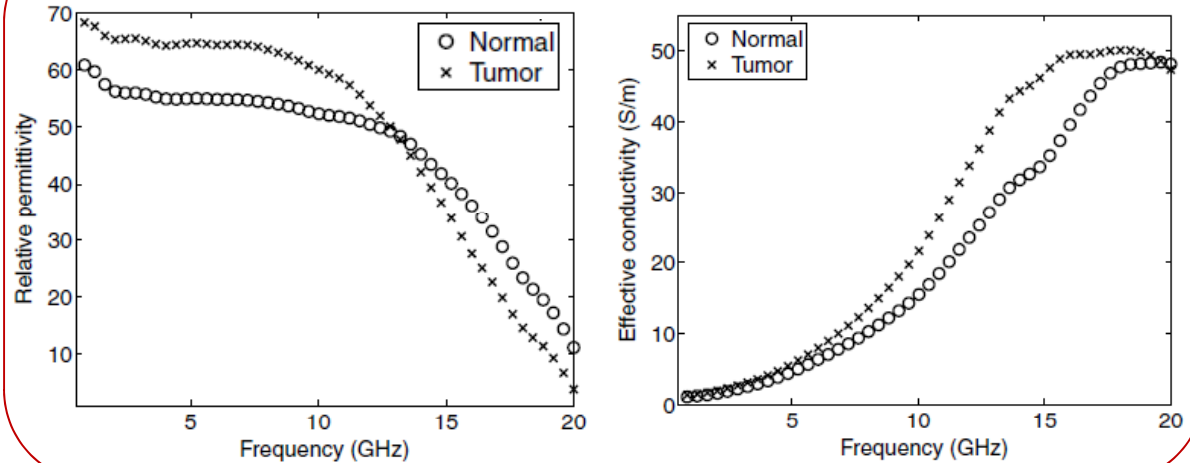
$$\sigma_{ev_malignant} > \sigma_{ev_normal} \text{ (18\%)}$$

Malignant tissues present higher values than the normal tissues due to a higher water content in the malignant tissues. The *in vivo* values are higher than the values *ex vivo*, due to a reduction in tissues temperature. Increasing the frequency, the relative permittivity decreases and the effective conductivity decreases.

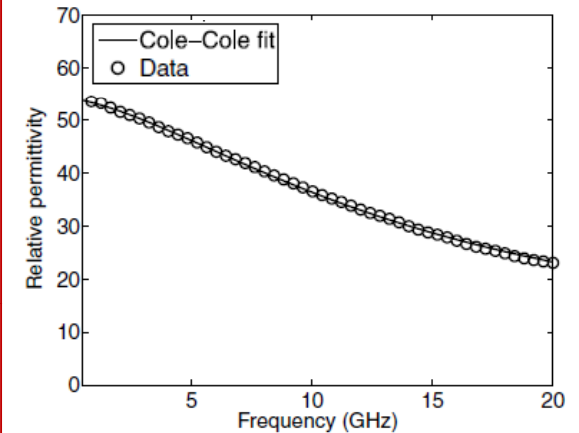
Wideband data analysis – 0.5-20GHz

Data for patient 5:

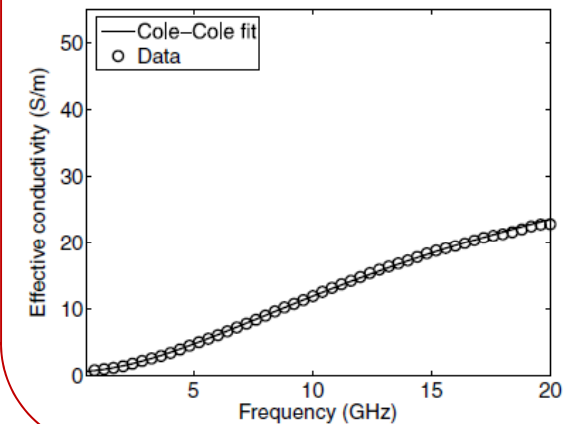
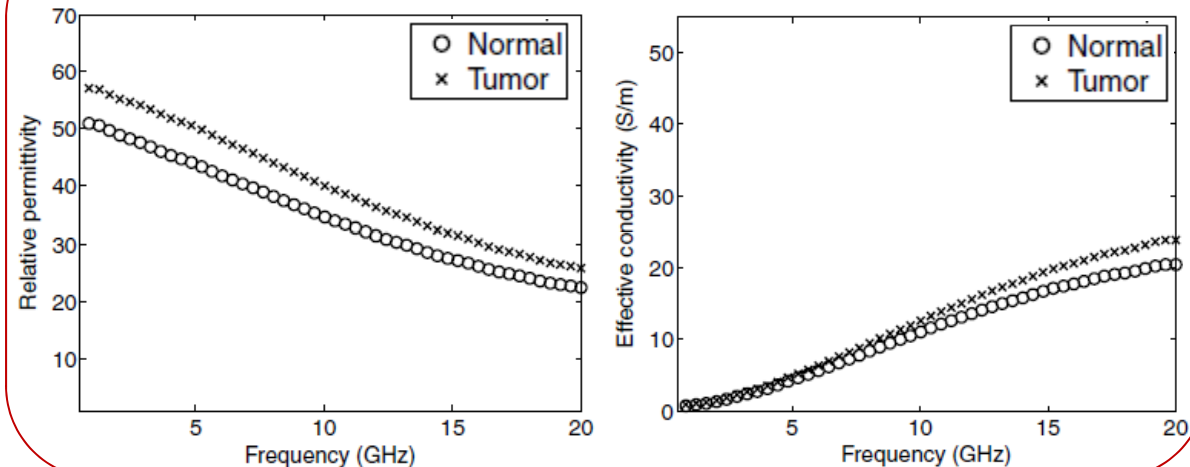
In vivo



Cole-Cole fit Normal tissue



Ex vivo



Differences between *in vivo* and *ex vivo* tissue properties are commonly attributed to variation in tissue temperature and water content. For *in vivo* different trends (at high frequencies) there are two explanations: experimental artifacts and biophysical phenomena.

Conclusions

- Dielectric properties characterization is important to differentiate malignant tissue against the normal ones.
- Differences between malignant and normal tissues need to be taken into account in electromagnetic and thermal models for hepatic microwave ablation, and should allow for the design of improved antennas.

Glucose-dependent dielectric properties of blood plasma

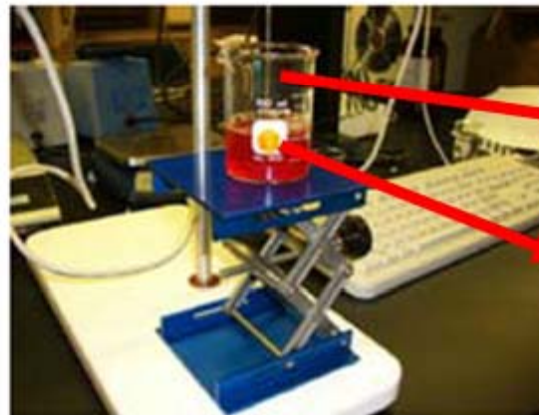
- The development of a reliable continuous glucose monitoring technology, which would lessen the complications associated with diabetes through optimal glycemic control, is a key to improving the lives of patients living with the disease.
- Considerable progress has been made in developing implantable biosensors that can continually monitor glucose levels. Functional operation time of commercial biosensors is only 10 days after the implantation due to the degradation and fouling of the sensor, and the changes in the tissue surrounding the sensor such as fibrosis and inflammation.
- **A correlation between electrical parameters (relative permittivity and conductivity) of blood plasma and plasma glucose concentration has been demonstrated and could be used to implement a microwave sensor (antenna) to predict glucose concentration within a given plasma sample (on the basis of antenna resonance variations).**

Study: • measurements on blood samples collected from 10 adults (age between 18 and 40).
• an Agilent dielectric kit and a VNA (vector network analyzer) were used for measurements between 500MHz and 20GHz.

Blood plasma samples



Measurement setup



slim probe

blood plasma sample



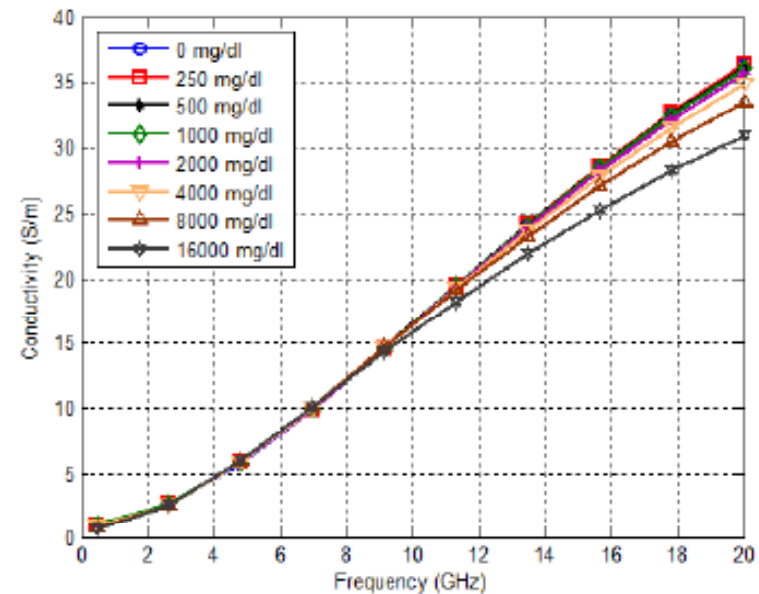
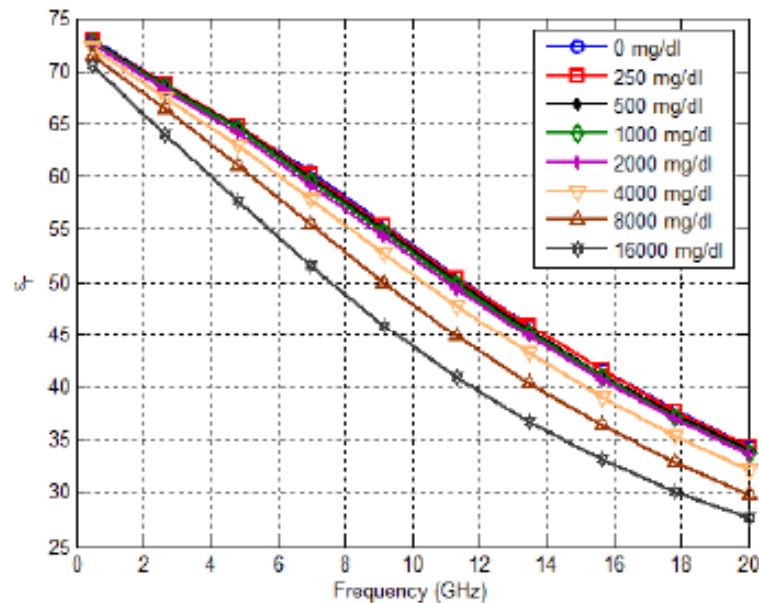
Methodology

- In a diabetic patient: glucose concentration varies between 30mg/dl and 400mg/dl;
- It has been assumed that changes in other minerals in blood plasma such as calcium, chloride, potassium and magnesium will have minor or no effects on the electrical properties (Na varies between 310mg/dl to 333mg/dl; Cl varies between 337mg/dl to 372mg/dl). During the study the blood glucose concentrations in the collected samples are manipulated *in-vitro*; therefore the concentration of other minerals in a specific sample remained unchanged during measurements.
- Initially, the glucose level is reset to zero for each sample, then each sample is measured at eight different glucose concentrations: 0mg/dl, 250mg/dl, 500mg/dl, 1000mg/dl, 2000mg/dl, 4000mg/dl, 8000mg/dl, 16000mg/dl.
- Wideband dielectric properties at each glucose concentration (averages for 10 samples, for each glucose concentration) are fitted to a single-pole Cole-Cole model (broadening distribution parameter α is fixed at 0.1).

Single-pole Cole-Cole model parameters at 500MHz-20GHz for 8 different glucose concentrations

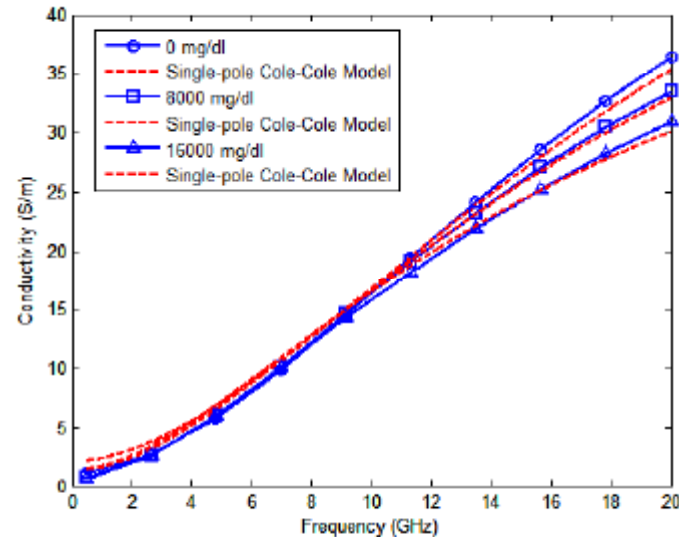
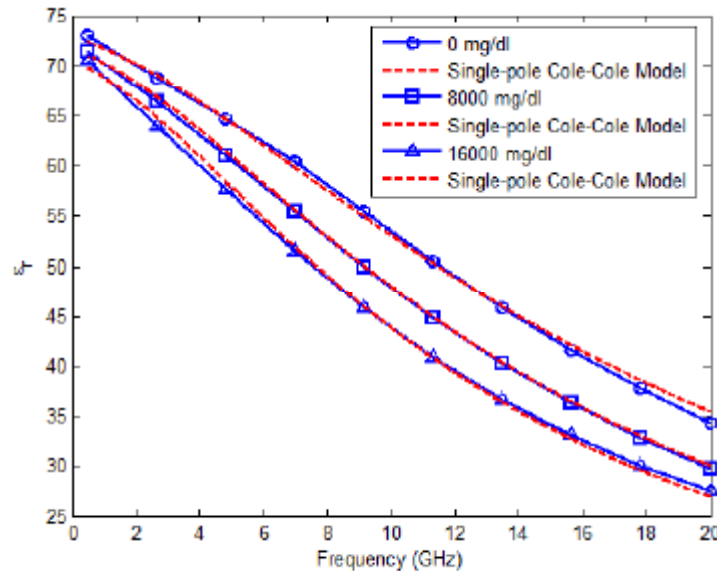
| | 0mg/dl | 250mg/dl | 500mg/dl | 1000mg/dl | 2000mg/dl | 4000mg/dl | 8000mg/dl | 16000mg/dl |
|------------------------|--------|----------|----------|-----------|-----------|-----------|-----------|------------|
| ϵ_{∞} | 2.8 | 2.04 | 2.67 | 2 | 2.11 | 3.1 | 3.29 | 5.63 |
| $\Delta\epsilon$ | 70.02 | 70.72 | 70.41 | 70.85 | 70.81 | 69.08 | 68.37 | 64.87 |
| $\tau(\text{ps})$ | 8.68 | 8.62 | 8.88 | 8.86 | 9.32 | 9.51 | 10.57 | 12.6 |
| $\sigma_s(\text{S/m})$ | 2.13 | 1.96 | 1.93 | 1.73 | 1.46 | 1.66 | 1.31 | 1.38 |

Dielectric constant & conductivity from 500MHz-20GHz



The dielectric constant and the conductivity decrease when glucose concentration in the sample increases. Differences are more visible at the higher frequency range.

Data fit single-pole Cole-Cole model



$$\tilde{\epsilon}(\omega, g) = \epsilon_{\infty} + \frac{\Delta\epsilon}{1 + (j\omega\tau)^{(1-\alpha)}} - j \frac{\sigma_s}{\omega\epsilon_0},$$

g : glucose concentration

$$\epsilon_{\infty}(g) = a_1 g^2 + b_1 g + c_1$$

$$\Delta\epsilon(g) = a_2 g^2 + b_2 g + c_2$$

$$\tau(g) = a_3 g^2 + b_3 g + c_3$$

$$\sigma_s(g) = a_4 g^2 + b_4 g + c_4$$

The data at each glucose level are fitted to a Cole-Cole model, and a second-order polynomial is used to model the glucose concentration dependence of the Cole-Cole-parameters (polynomial coefficients are estimated through a particle swarm optimization technique).

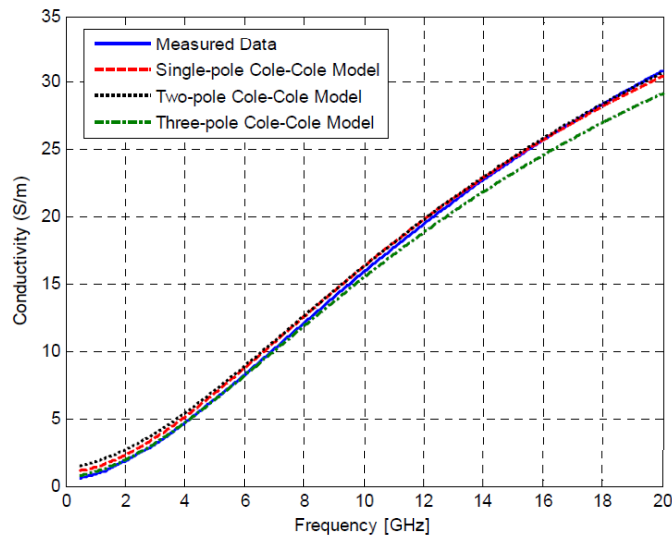
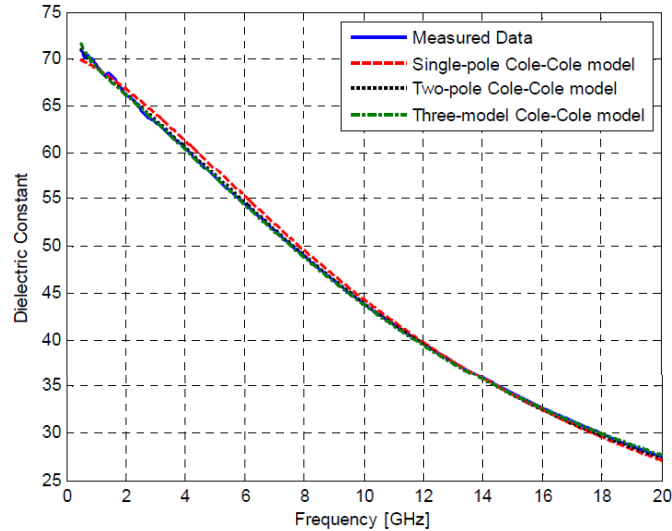
Then it will be possible to calculate the dielectric properties of the blood plasma at each glucose concentration, for any frequency between 500MHz and 20GHz..

17/11/2011

[10] Topsakal et al, Proceedings of XXX Int. Symp. URSI, August 2011.

Data fit for higher-order Cole-Cole models

The dielectric properties of a blood plasma sample with a glucose concentration of 500mg/dl are fitted to single-pole, two-pole and three-pole Cole-Cole model.



| | Single-pole | Two-pole | Three-pole |
|---------------------|-------------|----------|------------|
| ϵ_{∞} | 4.72 | 3.58 | 7.15 |
| $\Delta\epsilon_1$ | 65.95 | 64.14 | 63.33 |
| τ_1 (ps) | 12.2 | 11.55 | 12.12 |
| $\Delta\epsilon_2$ | | 4913.82 | 3632.97 |
| τ_2 (ns) | | 143.99 | 172.98 |
| $\Delta\epsilon_3$ | | | 256744 |
| τ_3 (μ s) | | | 156.74 |
| σ_s (S/m) | 1.02 | 0.88 | 0.28 |

A single-pole Cole-Cole model is sufficient to represent the measured data with less number of parameters and computational time.

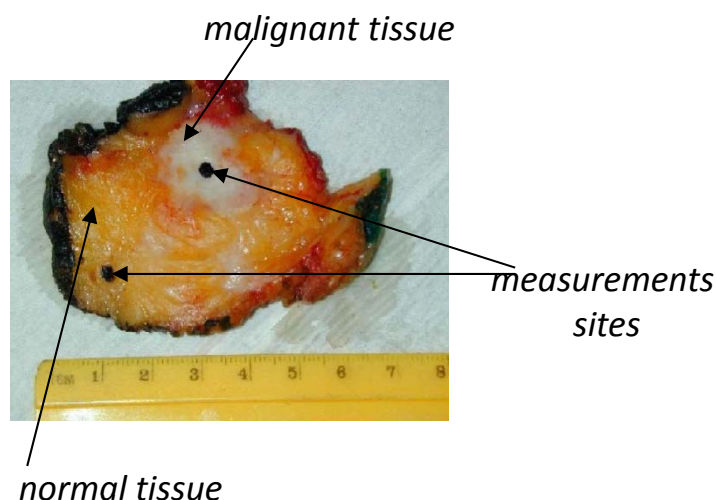
Conclusions

- For a given glucose concentration dielectric properties of any plasma sample can be derived.
- This is useful for designing electromagnetic sensors (whose resonances depend on the electrical parameters of the surrounding material) to estimate plasma glucose concentration.

Dielectric properties of breast tissues (0.5-20 GHz)

➤ The development of microwave breast cancer detection and treatment techniques has been driven by reports of substantial contrast in the dielectric properties of malignant and normal breast tissues.

- Study:**
- dielectric properties of normal and malignant breast tissue samples obtained from cancer surgeries were measured using an open-ended coaxial probe
 - probe diameter=3mm, probe sensing depth around 1-3 mm ensuring that the probe interrogates a small tissue volume).
 - a single-pole Cole-Cole model was used to fit complex permittivity data set of each sample.

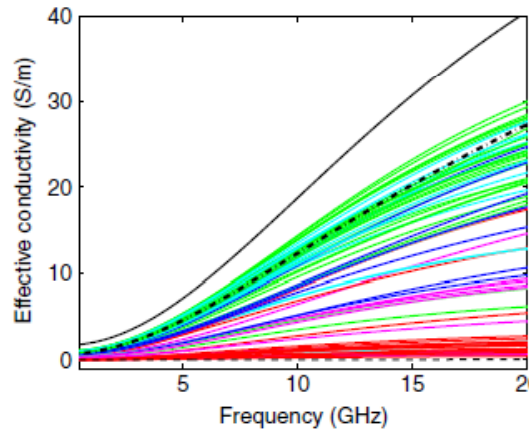
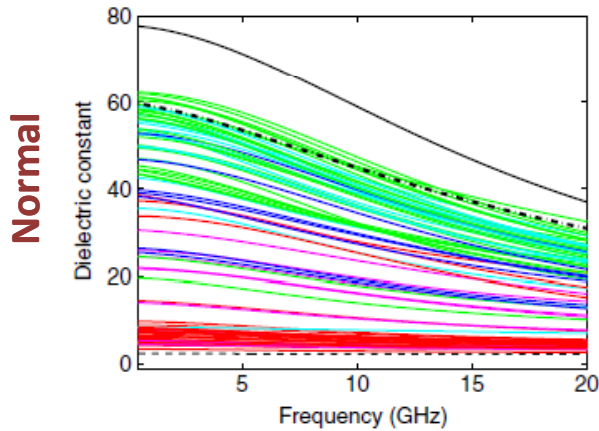


| | |
|--|---|
| Total number of patients | 196 |
| Total number of samples | 319 |
| Patient age | 35-87 (first group) 19-90 (second group) |
| Time from excision to measurements | 20-221min 11-240min |
| Tissue temperature during measurements | 18°C-25.7°C 19.9°C-27.2°C |

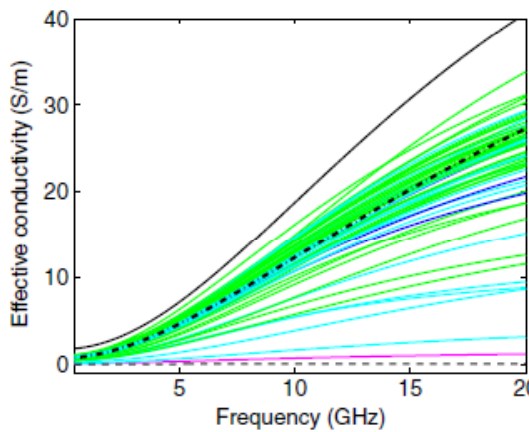
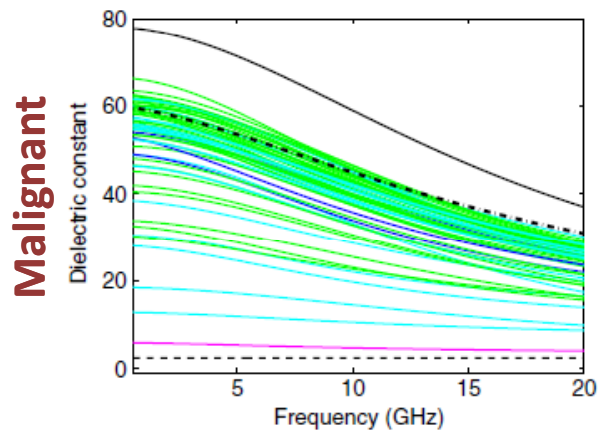
M. Lazebnik, D. Popovic, L. McCartney, C.B. Watkins, M.J. Lindstrom, J. Harter, S. Sewall, T. Ogilvie, A. Magliocco, T. M. Breslin, W. Temple, D. Mew, J.H. Booske, M. Okoniewski, S.C. Hagness, "A large-scale study of the ultrawideband microwave dielectric properties of normal, benign and malignant breast tissues obtained from cancer surgeries", *Phys. Med. Biol.* 52 (2007) 6093-6115



Normal vs. malignant breast tissues



- Most of the red curves (high adipose-content samples) cluster towards the low dielectric-properties end, while most of the green curves (low adipose-content samples) cluster towards the high dielectric properties end.
- The water content of normal breast tissues varies between very low water-content (high adipose content) and very high water-content (low adipose content).



- The cancer samples are “mostly” green (low adipose content).
- The water content of malign breast tissues is high.

Measured data

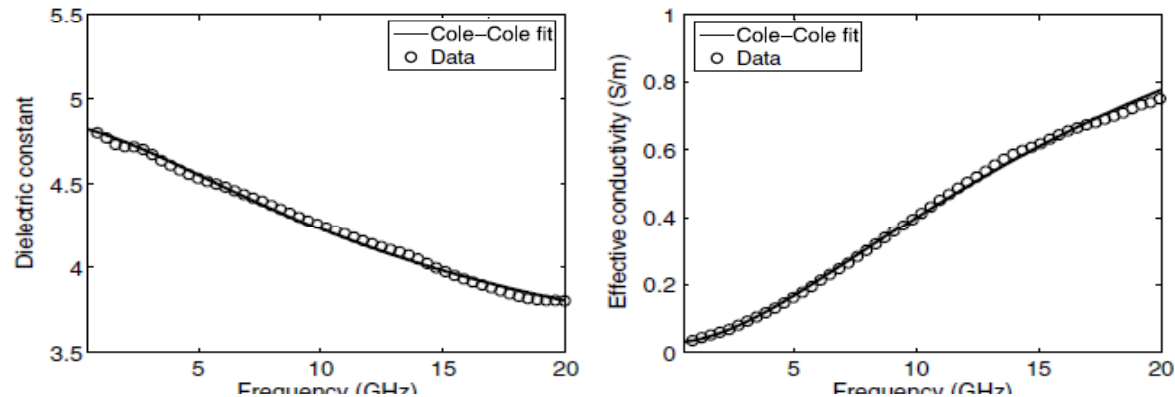
| | | | | |
|-------------------------|--------|------|------|------------------------|
| Highest adipose content | | | | Lowest adipose content |
| | | | | |
| Red | Purple | Blue | Cyan | Green |

Reference

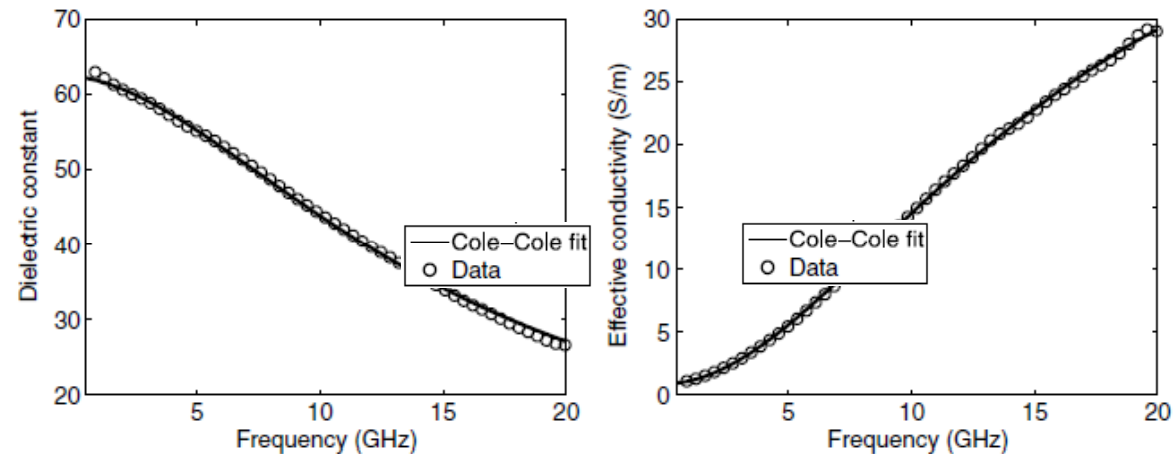
| | | |
|------------------------------|------------------------|-----------------------|
| Highest water content | | Lowest water content |
| | | |
| Saline solution (solid line) | Blood (dash-dot lines) | Lipids (dashed lines) |

Cole-Cole model for normal and cancer tissue samples

Normal tissue (*with* high adipose content)



Cancer tissue



The contrast in the microwave-frequency dielectric properties between malignant and normal adipose-dominated tissues in the breast is considerable, as large as 10:1.

On the other hand, the contrast in the microwave-frequency dielectric properties between malignant normal glandular/fibroconnective tissues in the breast is no more than about 10 %.

Conclusions

6106

M Lazebnik *et al*

Table 2. Cole–Cole parameters for the dielectric properties of the three adipose-defined groups of normal samples obtained from reduction surgeries.

| Percentile | Group 1 | | | Group 2 | | | Group 3 | | |
|----------------------------|---------|-------|-------|---------|-------|-------|---------|-------|-------|
| | 25th | 50th | 75th | 25th | 50th | 75th | 25th | 50th | 75th |
| ϵ_{∞} | 9.941 | 7.821 | 6.151 | 8.718 | 5.573 | 5.157 | 2.908 | 3.140 | 4.031 |
| $\Delta\epsilon$ | 26.60 | 41.48 | 48.26 | 17.51 | 34.57 | 45.81 | 1.200 | 1.708 | 3.654 |
| τ (ps) | 10.90 | 10.66 | 10.26 | 13.17 | 9.149 | 8.731 | 16.88 | 14.65 | 14.12 |
| α | 0.003 | 0.047 | 0.049 | 0.077 | 0.095 | 0.091 | 0.069 | 0.061 | 0.055 |
| σ_s ($S\ m^{-1}$) | 0.462 | 0.713 | 0.809 | 0.293 | 0.524 | 0.766 | 0.020 | 0.036 | 0.083 |

Table 3. Cole–Cole parameters for the dielectric properties of the three adipose-defined groups of normal samples obtained from cancer surgeries.

| Percentile | Group 1 | | | Group 2 | | | Group 3 | | |
|----------------------------|---------|-------|-------|---------|-------|-------|---------|-------|-------|
| | 25th | 50th | 75th | 25th | 50th | 75th | 25th | 50th | 75th |
| ϵ_{∞} | 5.013 | 7.237 | 7.816 | 3.891 | 6.080 | 6.381 | 3.122 | 3.581 | 3.882 |
| $\Delta\epsilon$ | 40.60 | 46.00 | 50.21 | 4.113 | 19.26 | 32.30 | 2.133 | 3.337 | 5.020 |
| τ (ps) | 10.16 | 10.30 | 10.47 | 13.83 | 11.47 | 10.41 | 14.27 | 15.21 | 12.92 |
| α | 0.091 | 0.049 | 0.055 | 0.038 | 0.057 | 0.081 | 0.099 | 0.052 | 0.059 |
| σ_s ($S\ m^{-1}$) | 0.607 | 0.808 | 0.889 | 0.082 | 0.297 | 0.561 | 0.034 | 0.053 | 0.103 |

- Group 1: 0-30% adipose tissue (high-water-content group)
- Group 2: 31-84% adipose tissue
- Group 3: 85-100% adipose tissue (low-water-content group)

The compact Cole-Cole representation for the wideband dielectric properties allow accurate dielectric properties values into future **numerical and experimental breast phantoms** used in the development of microwave breast imaging and breast cancer detection, monitoring and treatment applications.

17/11/2011

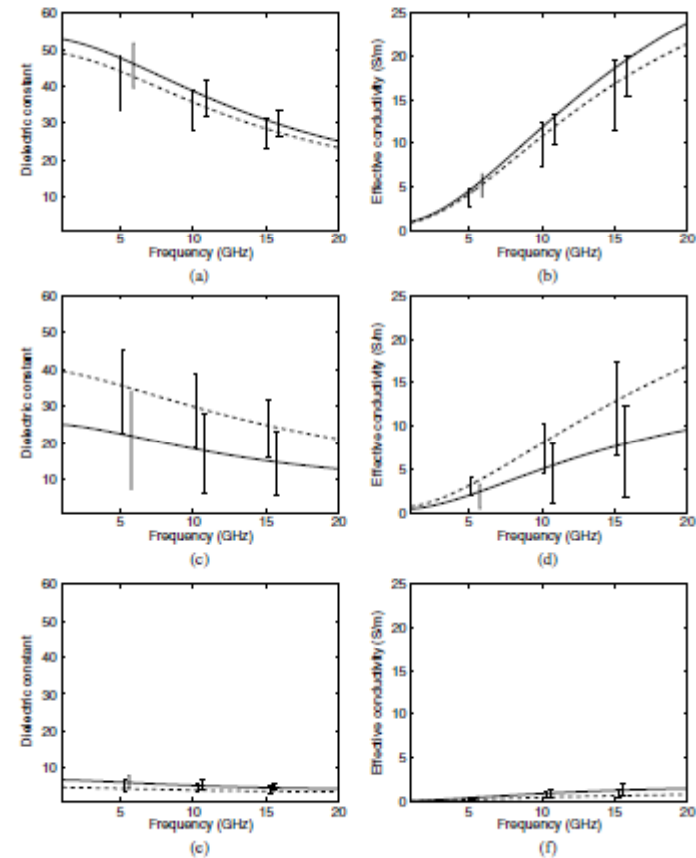


Figure 9. Median Cole–Cole curves for the dielectric properties of three adipose-defined tissue groups for the normal breast tissue samples obtained from reduction surgeries (dashed lines) and cancer surgeries (solid lines): (a) and (b) group 1 dielectric constant and effective conductivity; (c) and (d) group 2; (e) and (f) group 3.

References

1. C. Gabriel, S. Gabriel, E. Corthout, "The dielectric properties of biological tissues: I. Literature survey", *Phys. Med. Biol.* 41 (1996) 2231-2249.
2. S. Gabriel, R. W. Lau, C. Gabriel, "The dielectric properties of biological tissues: II. Measurements in the frequency range 10Hz to 20GHz", *Phys. Med. Biol.* 41 (1996) 2251-2269.
3. S. Gabriel, R. W. Lau, C. Gabriel, "The dielectric properties of biological tissues: III. Parametric models for the dielectric spectrum of tissues", *Phys. Med. Biol.* 41 (1996) 2271-2293.
4. P. Bernardi, S. Pisa, "Caratteristiche elettriche principali dei tessuti biologici", *Dispense Corso "Strumentazione Biomedica III"*.
5. G. Williams, D. K. Thomas, "Phenomenological and molecular theories of dielectric and electrical relaxation", *Novocontrol Application Note Dielectrics*, 1998.
6. K.R. Foster, H. P. Schwan, "Dielectric properties of tissues and biological materials: A critical review", *Bioengineering* 17 (1) (1989) 25-104.
7. <http://niremf.ifac.cnr.it/tissprop/htmlclie/htmlclie.htm>
8. A.P. O'Rourke, M. Lazebnik, J.M. Bertram, M.C. Converse, S.C. Hagness, J.G. Webster, D.M Mahvi, "Dielectric properties of human normal, malignant and cirrhotic liver tissue: *in vivo* and *ex vivo* measurements from 0.5 to 20GHz using a precision open-ended coaxial probe", *Phys. Med. Biol.* 52 (2007) 4707-4719.
9. D. Popovic, L. McCartney, C. Beasley, M. Lazebnik, M. Okoniewski, S.C. Hagness, J.H. Booske, "Precision open-ended coaxial probes for *in vivo* and *ex vivo* dielectric spectroscopy of biological tissues at microwave frequencies", *IEEE trans. On Microwave Theory and Tech.*, vol. 53 (5), May 2005.
10. E. Topsakal, T. Karacolak, E.C. Moreland, "Glucose-dependent dielectric properties of blood plasma", *Proceedings of XXX Int. Symp. URSI*, August 2011.
11. T. Karacolak, E.C. Moreland, E. Topsakal, "Cole-Cole model for glucose-dependent dielectric properties of blood plasma for continuous glucose monitoring", *Proceedings of XXX Int. Symp. URSI*, August 2011.
12. M. Lazebnik, D. Popovic, L. McCartney, C.B. Watkins, M.J. Lindstrom, J. Harter, S. Sewall, T. Ogilvie, A. Magliocco, T. M. Breslin, W. Temple, D. Mew, J.H. Booske, M. Okoniewski, S.C. Hagness, "A large-scale study of the ultrawideband microwave dielectric properties of normal, benign and malignant breast tissues obtained from cancer surgeries", *Phys. Med. Biol.* 52 (2007) 6093-6115.